Evaluation of the long-term performance of the deep U-type borehole heat exchanger on different geological parameters using the Taguchi method

Jinghua Jiang[a], Fenghao Wang[a,*], Xiong Yang[a], Yuping Zhang[b], Jiewen Deng[c], Qingpeng Wei[c], Wanlong Cai[a,**], Chaofan Chen[d]

[a]*School of Human Settlements and Civil engineering, Xi'an Jiaotong University, Xi'an, Shaanxi 710049, China*
[b]*Key Laboratory of Coal Resources Exploration and Comprehensive Utilization, Ministry of Natural Resources, Xi'an, Shaanxi 710021, China*
[c]*Department of Building Science, Tsinghua University, Beijing 100084, China*
[d]*Helmholtz Center for Environmental Research-UFZ, Permoserstraße 15, 04318 Leipzig, Germany*

Abstract

In recent years, deep geothermal energy has become a solid option for building heating worldwide. For the densely populated urban area, a novel closed-loop system of the deep U-type borehole heat exchanger (DUBHE) has attracted attention in northern China. In order to achieve the evaluation of geological parameters on the long-term performance of DUBHE, thermal conductivity, geothermal gradient, specific heat capacity, groundwater flow direction, and Darcy velocity are selected in this paper and all the parameters are set in three levels. And orthogonal test $L_{18}(3^5)$ is established by adopting the Taguchi method for the reduction of simulation time cost. Three evaluation indexes are introduced to investigate the impacts of geological parameters on the performance of DUBHE and obtain the optimal set, including average outlet temperature T_{out}, maximum cumulative heat extraction amount Q_{total} and soil temperature decay rate D_{soil}. Results show that the geothermal gradient has the most significant effect on T_{out} and

*Corresponding author
**Corresponding author
Email addresses: jiang1998@stu.xjtu.edu.cn (Jinghua Jiang), fhwang@mail.xjtu.edu.cn (Fenghao Wang), 18205205239@stu.xjtu.edu.cn (Xiong Yang), xazyp@163.com (Yuping Zhang), dengjw16@mails.tsinghua.edu.cn (Jiewen Deng), qpwei@tsinghua.edu.cn (Qingpeng Wei), cwl828@stu.xjtu.edu.cn (Wanlong Cai), chaofan.chen@ufz.de (Chaofan Chen)

Q_{total}, and its contribution degree is 70.14% and 62.10% respectively. As for the D_{soil} index, the most influential parameter is specific heat capacity and the corresponding contribution ratio is 92.41% determined by the analysis of variance (ANOVA) method. For the optimized combination by adopting matrix analysis, the T_{out} reaches 33.92 °C, the Q_{total} is 284.08 TJ and the D_{soil} of the optimized scenario is 12.66% after the long-term operation. In addition, according to the orthogonal test results, this study intuitively discusses the potential of carbon emission reduction for the DUBHE under the typical geological conditions in northern China. The study results presented in this work can guide the system design of DUBHE and serve as the reference for the decision-maker in the application of deep geothermal heating technology.

Keywords: Deep U-type borehole heat exchanger (DUBHE); Long-term performance; Geological parameters; Taguchi method; Evaluation index

---

Nomenclature

Roman letters

c	specific heat capacity ($\mathrm{J\,kg^{-1}\,K^{-1}}$)
H	heat sink/source term ($\mathrm{W\,m^{-3}}$)
$\mathbf{I}$	identity matrix (-)
D	decay rate of soil temperature (-)
L_1	length of descending/ascending pipe (m)
L_2	length of horizontal pipe (m)
m	number of factor levels (-)
n	total number of experiments (-)
r	repeated number of each level experiment(-)
d	pipe diameter(m)
i	number of sample iterations(-)
Q	heat extraction (TJ)

q_n heat flux ($\mathrm{W\,m^{-2}}$)

y simulated result

T temperature (°C)

t time (s)

$\mathbf{v}$ vector of flow velocity ($\mathrm{m\,s^{-1}}$)

Greek Letters

ϵ rock/soil porosity (-)

β_L longitudinal heat dispersivity (m)

$\mathit{\Gamma}$ boundary

λ thermal conductivity ($\mathrm{W\,m^{-1}\,K^{-1}}$)

$\mathit{\Lambda}$ thermal hydrodynamic dispersion tensor($\mathrm{W\,m^{-1}\,K^{-1}}$)

$\mathit{\Phi}$ thermal resistance ($\mathrm{m^2\,K/W}$)

ρ density ($\mathrm{kg\,m^{-3}}$)

Operators

Δ difference operator

∇ nabla vector operator

$\sum$ integral operator

Subscripts

f circulation fluid

g grout

s soil

w groundwater

Abbreviations

ANOVA Analysis of Variance

BHE Borehole Heat Exchanger

DBHE Deep Borehole Heat Exchanger

DC-FEM Dual Continuum Finite Element Method

DCBHE Deep Coaxial Borehole Heat Exchanger

DOF Degrees of Freedom

DUBHE Deep U-type Borehole Heat Exchanger

FDM Finite Difference Method

GSHP Ground Source Heat Pump

S/N Signal to Noise

SS Sum of the Squares of the deviations

V Variance

1. Introduction

Energy production and supply are important factors restricting the development of society and are directly related to the lifeblood of countries worldwide [1]. In 2018, the Intergovernmental Panel on Climate Change of the United Nations (IPCC) has clearly stated that the global temperature rise will be limited around 1.5 °C [2] by the end of the century in the climate change assessment report. In order to limit global warming and enhance the realization for green and sustainable development, countries all over the world are committed to the utilization of renewable energy for the low-carbon energy transition [3]. It is worth noting that building energy consumption accounts for the largest proportion of global energy consumption [4] and contributes to more than 40% [5] [6] of the total primary energy consumption in the European Union. Focusing on space heating in building sector, the proportions reach 60%∼80% [7] and 40% [8] of the energy consumption in Europe and China, respectively. Therefore, the renewable energy transition for building heating in order to reduce energy consumption has become a key part of achieving the carbon neutral goal [9].

The geothermal resource is a kind of clean, low-carbon, and renewable resource with huge reserve contained in the subsurface. It is widely used for versatile purposes, such as power generation, building heating, and agriculture [10]. Considering the heat exchange capacity of a single shallow BHE in Ground Source Heat Pump (GSHP) systems, a concept of deep coaxial borehole heat exchanger (DCBHE) was proposed by Rybach [11] to obtain higher heat extraction capacity. For the DCBHE, an earliest field test was reported in Hawaii [12], and later there were pilot applications in Aachen, Germany [13] and Shaanxi Province, China [14]. There have been many studies reported concerning DCBHE, including the field test [15] and numerical analysis [16, 17, 18]. Both experimental data and simulated results show that one single DCBHE with the depth of 2500 m can extract about 300 kW heat amount for building heating.

To get better heat extraction performance, a new type of deep U-type borehole heat exchanger (DUBHE) has been proposed for building heating in northern China recently [19, 20]. As for the DUBHE, it has a single-pipe structure, which involves two vertical pipes with thousand-meter depth and a horizontal section connecting vertical boreholes. The circulation fluid in DUBHE flows through descending well, horizontal well and ascending well successively, forming a closed-loop circulation to extract deep geothermal energy. The schematic diagram of DUBHE can be seen in Fig. 1.

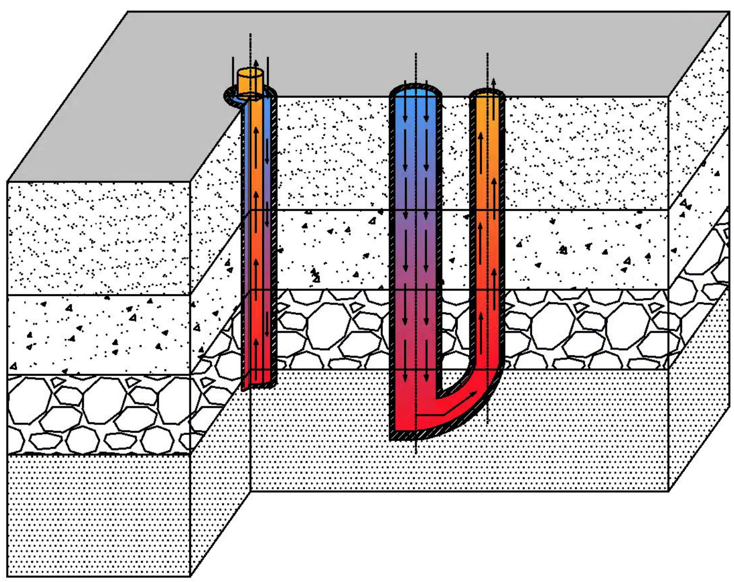

Figure 1: Schematic diagram of deep borehole heat exchanger: left, DCBHE; right, DUBHE

In scientific studies, numerical approach is usually chosen by researchers to conduct related research for DUBHE because of the convenient on handling the complex boundary conditions. For instance, FLUENT [21], OpenGeoSys [22] software and Finite Difference Method (FDM) [23] have been used for the heat extraction performance analysis and parameter optimization of DUBHE. Several foreign researchers focus on the transformation of abandoned oil Wells into BHE [24] [25]. In Hinton, a model of DUBHE was established to investigate the feasibility of retrofitting an abandoned oil well with DUBHE to extract geothermal energy in the Western Canadian Sedimentary Basin near Hinton [26]. Gharibi et al. [27] proved that the extracted geothermal energy from an abandoned oil well retrofitted with a DUBHE can be used for direct applications in Iran, and even electricity generation under the condition of 0.01m pipe diameter, 303.16K inlet temperature and 0.5m/s inlet velocity (circulation fluid is water). Domestic researchers mainly study and optimize the performance of DUBHE. For instance, S. Tang [28] conducted detailed numerical investigations on the performance of horizontal section of the DUBHE, and found that the heat extraction rate can be optimal when the circulation flow rate is 33.85 t/h. Wang [29] found that the inlet temperature for the DUBHE of 2000 m depth increased by 10.46 °C when the geothermal gradient increased from 20 °C/km to 30 °C/km. Li et al. [30] discussed the influence of design parameters, geological parameters and operation parameters on the heat extraction performance of DUBHE. And the contribution degree of each influencing factor to the system performance are quantified.

Based on the current research status, geological parameters and groundwater seepage [31] have an obvious impact on the long-term heat extraction performance of DUBHE. There will be a corresponding series of scientific questions when systematically analyzing the influence of geological parameters including groundwater seepage on the performance of DUBHE: 1) What is the difference in heat extraction performance of DUBHE under different geological conditions? 2) How to quantify the significance of influence and contribution of factors on the heat extraction performance of DUBHE during the long-term operation? 3) And where are the advantages of the DUBHE system compared with the common heating system using fossil fuels in northern China? In order to solve above three scientific questions, Taguchi method will be introduced in this study. Taguchi method was proposed by Genichi Taguchi [32], which has the advantages of high efficiency and economy in calculation. And this method is often used to quantify and evaluate the affect of parameters on the system performance [33], especially in the field of geothermal energy utilization. The existing researches mostly use Taguchi method to optimize the performance of GSHP system, including single U-tube BHE [34], double U-tube BHE [35] and helical heat exchanger [36]. Thus, the Taguchi method is selected to conduct the quantitative analysis for long-term performance of DUBHE.

Overall, this paper establishes DUBHE model by OpenGeoSys software and conducts a series of long-term simulation of DUBHE. Then the Taguchi method is used to answer the scientific questions. The related content is organized as follows: Section 2 introduces the governing equation for DUBHE model in OpenGeoSys and describes the model verification results. Specific details of DUBHE parameters and step size of model are given in section 3. Section 4 introduces the Taguchi method, and 18 sets of orthogonal test conditions $L_{18}(3^5)$ are made based on five factors and corresponding three levels. By adopting the signal-to-noise (S/N) ratio, matrix analysis and analysis of variance (ANOVA), the significance and contribution ratio of influencing factors for the long-term performance of DUBHE are evaluated and quantified by analyzing three evaluation indexes $\mathrm{T_{out}}$, $\mathrm{Q_{total}}$, and $\mathrm{D_{soil}}$ of the DUBHE system. And the corresponding results are shown in section 5. Case study including carbon emission reduction analysis of DUBHE and future prospects are presented in section 6. This paper ends with a brief summary and main conclusions in section 7.

2. Methodology

2.1. Governing equations

In this study, the OpenGeoSys software, which adopts the Dual-continuum Finite Element Method (DC-FEM) [37, 22], is used for the simulation of DUBHE. According to the DC-FEM method, the soil is discretized by 3D elements in a prism form, while the borehole part (including both DUBHE and surrounding grout) is simplified as one-dimensional line elements. The coupling boundary between these two parts depends on the the Robin-type boundary condition of heat flux [38]. By imposing the governing equations on both the borehole part and soil part, the DC-FEM method can mimic the dynamic heat transfer process among circulation fluid, borehole pipe, grout, and surrounding soil. Compared with the conventional numerical simulator, OpenGeoSys does not need to describe all the millimeter-level details within and beside the borehole heat exchanger. Consequently, the calculation cost will be considerably reduced and the long-term simulation for the DUBHE will be of feasibility. Considering that the complete governing equations have been introduced in the published study of DUBHE, we will not spend too much space on the introduction in this part, interested readers can refer to the literature [22].

2.2. Model verification

Based on OpenGeoSys software, there are a large number of model validation and verification cases reported in the previous publication conducted by our research group. In the aspect of shallow BHE, the BHE array model implemented by OpenGeoSys software has been verified against analytical solutions [39, 40] and validated with actual monitoring data from the Leicester's GSHP project [41]. As for the DBHE, the DCBHE and DUBHE model established by OpenGeoSys software have previously been verified against Beier's analytical solution [18, 42] and Ramey's analytical solution [22], respectively. Moreover, the simulated results of DCBHE have been validated by monitoring data from a pilot project in Xi'an [43]. Based on the sufficient monitoring data and analytical solutions, we believe that the previous work concerning verification of the BHE/DBHE models ensures the capability of OpenGeoSys software to simulate the long-term performance of DBHE within an acceptable calculation cost. Therefore, the OpenGeoSys software is chosen to calculate the heat extraction capacity of DUBHE under different geological parameters during long-term operation.

3. Model description

3.1. Model setup

In this study, the ascending and descending wells are perpendicular to the horizontal borehole and connected by the horizontal borehole at the bottom. According to a pilot project of DUBHE in northern China [20], the length of the descending and ascending wells are set as 2500 m, and the horizontal distance between them is 600 m. In order to avoid the thermal plume touching the lateral boundary during long-term operation, the size of the entire domain is set as $800 \times 200 \times 2700$ m. The entire model domain can be seen in Fig. 2 and the detailed parameters of the DUBHE are listed in Table 1. The soil properties are kept to be isotropic over the entire domain.

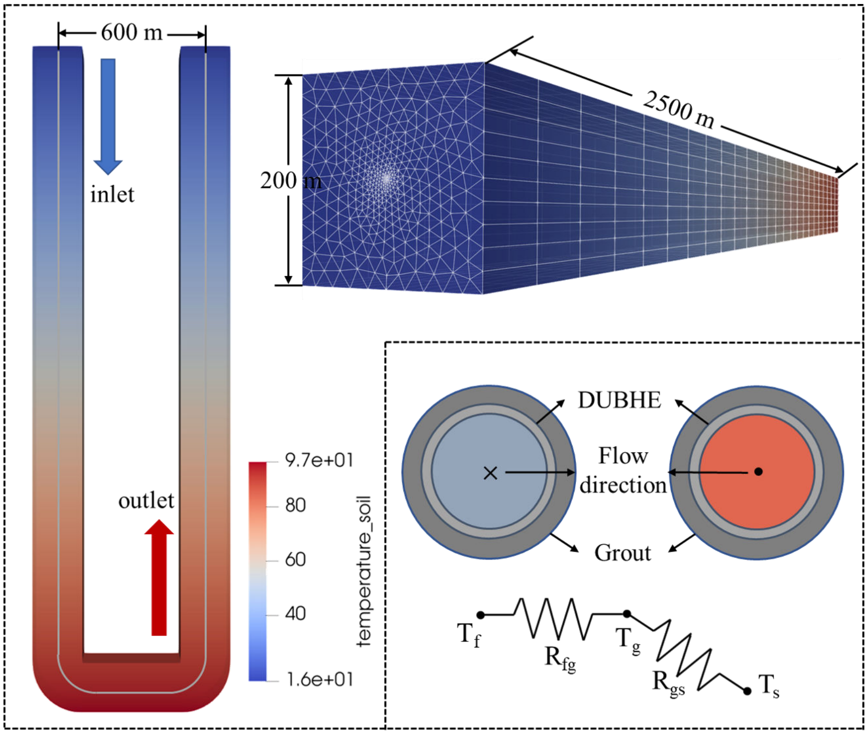

Figure 2: DUBHE 3D model domain in OpenGeoSys

Table 1: Detailed parameters of the DUBHE in numerical models

Item	Parameter	Value	Unit
Borehole	Borehole depth	2500	m
	Borehole diameter	0.2445	m
	Borehole spacing	600	m
	Outer diameter of tube	0.1594	m
	Wall thickness of tube	0.00919	m
	Thermal conductivity of tube wall	40	W m^{-1} K^{-1}
Grout	Density	2190	kg m^{-3}
	Specific heat capacity	1735.16	J kg^{-1} K^{-1}
	Thermal conductivity	1.2	W m^{-1} K^{-1}
Circulation fluid	Thermal conductivity	0.6	W m^{-1} K^{-1}
	Specific heat capacity	4190	J kg^{-1} K^{-1}
	Density	998	kg m^{-3}
	Dynamic viscosity	0.000931	kg m^{-1} s^{-1}
	flow rate	0.01389	m^3 s^{-1}

The previous study have shown that the fluctuation in surface temperature have little effect on the overall heat extraction of DBHE [18], so the top boundary of the soil domain is set to a Dirichlet-type boundary with constant surface temperature of 15.6 °C [44]. The lateral side of domain is adiabatic boundary, which is set as no-heat-flux condition in OpenGeoSys software. And the Neumann-type boundary with 60 mW/m^2 is set for the bottom of the domain to simulate the actual geothermal heat flux [43].

3.2. Grid independence test

For numerical simulation, grid independence test is needed to save calculation time, while the accuracy of simulated results can be guaranteed. According to the red points in Fig. 3, it can be seen that the step selected in the axial direction are 100 m of a layer, and the change of axial step size has little effect on the simulated outlet temperature of DUBHE. Considering the actual borehole diameter, the mesh size in the area near the DUBHE is 0.75m. The mesh size in the peripheral area is gradually sparse, and the radial step at the edge of DUBHE model is 20 m. After the axial and radial step size is determined, the number of nodes of the 3D numerical model in this paper is 37370. In order to ensure generate stable numerical results, the time step of the heating season gradually increased from 1 h (initial) to 12 h (one month later) according to the previous study [43]. And the time cost of running a heating season under constant inflow temperature boundary condition is 14 min by using HP Z6 G4 Workstation.

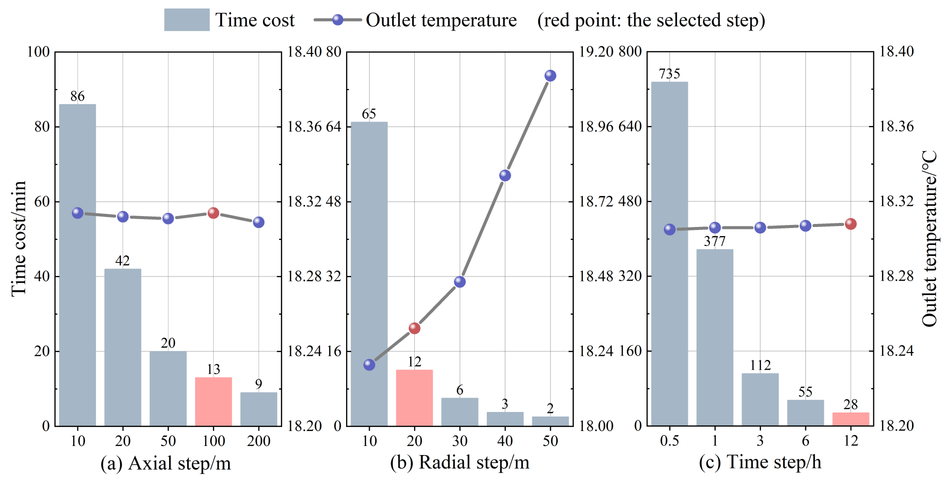

Figure 3: Outlet temperature of DUBHE and simulated time cost under different radial, axial density and time steps (after one heating season)

4. Orthogonal test design

4.1. Taguchi method

The analysis of influencing factors under multiple levels often faces the problem of redundant experiment conditions. At this time, it is necessary to select representative combinations for tests under various experimental conditions to reduce the calculation time. Taguchi method is widely used in engineering research because of its advantages of the balanced and dispersed test, simple data calculation and so on [45]. Based on the Taguchi method, this paper analyzes and evaluates the influence of geological parameters on the long-term performance of DUBHE, and the process is listed as follows:

★**Preparatory work**

1) Determine the geological influencing factors and the corresponding level;

2) Make the corresponding orthogonal experiment table;

3) Execute the simulation of various scenarios;

★**Post processing and analysis**

4) Select evaluation indexes;

5) Use S/N ratio to determine the significance of influencing factors;
6) Make average S/N ratio tables and draw related figures;
7) Use ANOVA method to determine the contribution of factors;
8) Make contribution rate tables and draw related figures.

Table 2 shows detailed information about the five geological parameters, including level parameters and thermal reservoir information. The related references are also cited in the specific position in Table 2.

Table 2: Influencing factors and their levels

	Factors	Unit		Levels		
				1	2	3
A	Thermal conductivity [46]	W m^{-1} K^{-1}	0-500m	1.2	1.6	1.8
			500-1300m	1.5	1.8	2.2
			1300-2000m	1.8	2.0	3.0
			>2000m	2.0	2.5	4.0
B	Geothermal gradient [47]	°C km^{-1}		20	30	40
C	Specific heat capacity [48]	J m^{-3} K^{-1}	0-500m	2.28×10^6	2.52×10^6	4.20×10^6
			500-1300m	2.00×10^6	2.32×10^6	4.00×10^6
			1300-2000m	1.72×10^6	1.97×10^6	3.60×10^6
			>2000m	1.70×10^6	1.96×10^6	3.56×10^6
D	Groundwater flow direction [49]			Counter	Parallel	Vertical
E	Darcy velocity [50]	m s^{-1}		2×10^{-9}	2×10^{-8}	2×10^{-7}

4.2. Objective functions

In this paper, three indexes, including T_{out}, Q_{total}, and D_{soil} are introduced to evaluate and quantify the heat extraction of DUBHE under different geological parameters both on short-term performance and long-term sustainability. The T_{out} index is defined as the average outlet temperature of DUBHE during the first heating season when the inlet temperature is 4 °C considering that the temperature threshold of the heat pump unit [51]. The Q_{total} index is determined by the maximum cumulative heat extraction amount of DUBHE during long-term operation, and its calculation reads,

$$Q_{total} = NQ_{average} \tag{1}$$

Where, $Q_{average}$ is the maximum heat extraction amount when the inlet temperature of DUBHE approaches 0 °C in the last heating season after long-term operation. N is operation years, and the value of N is 20 in this study.

The D_{soil} refers to the soil temperature decay rate compared with the initial temperature at the position 5 m away from the descending boreholes of DUBHE and 1250 m away from the surface. The concept of D_{soil} is defined as follows.

$$D_{soil} = \frac{T_{initial} - T_{soil}}{T_{initial}} \times 100\% \tag{2}$$

4.3. Post-processing method: signal-to-noise (S/N) ratio

In the post-processing of Taguchi method, 'the larger the better' [52] and 'the smaller the better' [53] are the most common functions. The former mode means that with a larger result of the objective function, the impact of factor is more significant, and so does the latter mode. Obviously, for the first two indicators, the larger the result, the better the influence of parameters [30]. For the D_{soil}, that is 'the smaller the better' objective function [54].

The relevant calculation formula is listed as follows:

The larger the better:

$$\frac{S}{N} = -10\lg\left(\frac{1}{i}\sum\frac{1}{y^2}\right) \tag{3}$$

The smaller the better:

$$\frac{S}{N} = -10\lg\left(\frac{1}{i}\sum y^2\right) \tag{4}$$

Where, i is the number of sample iterations, y is the simulated result for each scenario.

4.4. Post-processing method: analysis of variance (ANOVA)

ANOVA is a statistical model used to further evaluate the relative significance, the contribution of each factor, and error to the objective function. The essence of the ANOVA method is to analyze the significance of influence by constructing a statistical function F and using F_{test} under certain reliability levels [55]. The larger the F value is, the greater the contribution is. The calculation within ANOVA is presented as follows.

$$DOF = m - 1 \tag{5}$$

Where, DOF is the degree of freedom and m is the number of factor levels.

$$SS = \frac{1}{r}\sum_{i=1}^{m} K_{ij}^2 - \frac{\left(\sum_{i=1}^{n} y\right)^2}{n} \tag{6}$$

Where, SS is the sum of the squares of the deviations, K_{ij} is the sum of all the calculated results when the factor is i, y is the simulated result for each scenario.

$$r = \frac{n}{m} \tag{7}$$

Where, r is the repeated number of each level and n is the total number of experiments.

$$V = \frac{SS}{DOF} \tag{8}$$

Where, V is the variance.

Finally, the expression of a statistical function is constructed as follows:

$$F_{factor} = \frac{V_{facor}}{V_{error}} \tag{9}$$

5. Results

In this section, the long-term heat extraction performance of DUBHE under different geological parameters are investigated based on the orthogonal test. Table 3 shows the values and S/N ratios of $\mathrm{T_{out}}$, $\mathrm{Q_{total}}$, and $\mathrm{D_{soil}}$ of 18 orthogonal scenarios.

Table 3: T_{out}, Q_{total} and D_{soil} for DUBHE and the corresponding S/N ratios

Scenarios	Parameters					Results			S/N		
	A	B	C	D	E	T_{out}(°C)	Q_{total}(TJ)	D_{soil}(%)	T_{out}	Q_{total}	D_{soil}
1	1	1	1	1	1	27.10	111.97	14.34	28.66	40.98	16.87
2	1	1	2	2	3	27.01	114.05	13.68	28.63	41.14	17.28
3	1	2	1	3	3	28.99	152.41	14.20	29.24	43.66	16.95
4	1	2	3	1	2	28.56	159.67	11.78	29.12	44.06	18.58
5	1	3	2	3	2	30.71	188.70	13.75	29.75	45.52	17.23
6	1	3	3	2	1	30.50	196.99	11.63	29.69	45.89	18.69
7	2	1	1	3	2	27.69	127.53	14.82	28.85	42.11	16.58
8	2	1	3	1	3	27.22	134.78	11.87	28.70	42.59	18.51
9	2	2	2	2	2	29.63	172.11	14.24	29.43	44.72	16.93
10	2	2	3	3	1	29.35	180.40	12.05	29.35	45.12	18.38
11	2	3	1	2	3	31.74	213.58	14.87	30.03	46.59	16.55
12	2	3	2	1	1	31.67	214.62	14.25	30.01	46.63	16.92
13	3	1	2	3	1	28.96	165.89	14.83	29.24	44.40	16.58
14	3	1	3	2	2	28.61	169.00	12.15	29.13	44.56	18.31
15	3	2	1	2	1	31.58	214.62	15.15	29.99	46.63	16.39
16	3	2	2	1	3	31.52	217.73	14.46	29.97	46.76	16.80
17	3	3	1	1	2	34.11	269.57	15.23	30.66	48.61	16.35
18	3	3	3	3	3	33.94	290.30	12.34	30.61	49.26	18.17

5.1. Analysis of S/N ratio

Table 4, Table 5, and Table 6 show corresponding average S/N ratios of five geological parameters at three levels respectively. And the relevant data are shown in Fig. 4, Fig. 5 and Fig. 6.

According to Fig. 4, the significance of influence for T_{out} is in the order of B, A, C, E, and D (geothermal gradient, thermal conductivity, specific heat capacity, Darcy velocity, and groundwater flow direction). And the levels and S/N ratios for the factor giving the best T_{out} are specified as B_3(S/N=30.13), A_3(S/N=29.95), C_1(S/N=29.60), E_3(S/N=29.56) and D_1(S/N=29.55) respectively. For T_{out} index, the optimized combination is $A_3B_3C_1D_1E_3$.

Taking Q_{total} as the objective function, the significance of influence is in the order of B, A, C, E, and D (geothermal gradient, thermal conductivity, specific heat capacity, Darcy velocity, and groundwater flow direction). According to Fig. 5, the optimal parameters of five factors at three levels can be obtained, which are B_3(S/N=47.20), A_3(S/N=46.90), C_3(S/N=45.51), E_3(S/N=45.44), and D_1(S/N=45.33) respectively. And the corresponding optimized combination is $A_3B_3C_3D_1E_3$.

As for the D_{soil} index, the significance of influence is in the order of C, A, E, B, and D (specific heat capacity, thermal conductivity, Darcy velocity, geothermal gradient, and groundwater flow direction). According to the Fig. 6, the optimal parameters of five factors at three levels can also be obtained, which are C_3(S/N=18.44), A_1(S/N=17.57), E_3(S/N=17.35), B_1(S/N=17.32), and D_2(S/N=17.32) respectively. And the corresponding optimized combination is $A_1B_1C_3D_2E_3$.

According to Fig. 4 and Fig. 5, average S/N ratios of T_{out} and Q_{total} will have an increment with the increase of thermal conductivity. Thermal conductivity is used to measure the heat conduct ability. The higher the thermal conductivity is, the faster the heat transfer rate will be. The specific data show that, when the thermal conductivity is the level-1, the average T_{out} of DUBHE is 28.81 °C (S/N=29.19), and the average Q_{total} of DUBHE is 153.96 TJ (S/N=43.75). When the thermal conductivity is at the level-3, the above two indicators increase to 31.45 °C(S/N=29.95) and 221.18 TJ (S/N=46.90). The soil temperature decay rate decreases with the increase of thermal conductivity, which can be interpreted as the stronger heat recovery of the surrounding subsurface.

The larger the geothermal gradient, the higher the bottom temperature of the soil. Therefore, the average T_{out} and the average Q_{total} of DUBHE will increase with the increase of geothermal gradient. For example, when the geothermal gradient increases from 20°C km^{-1} to 40°C km^{-1}, T_{out} of DUBHE increases from 27.77 to 32.11 °C, which the increasing rate is 15.66% compared with level-1. And the average Q_{total} of DUBHE varies from 137.20 TJ(S/N=42.75) to 228.96 TJ(S/N=47.20) when the geothermal gradient increases from 20°C km^{-1} to 40°C km^{-1}. The soil temperature decay rate is less affected by geothermal gradient, and the average value of D_{soil} for the three levels is about 13.6%.

Thermal diffusivity is defined as the ratio of thermal conductivity to specific heat capacity, which is used to measure the ability of an object to achieve uniform temperature in the heat transfer process. With the same thermal conductivity, the thermal diffusivity of soil gradually decreases with the increase of specific heat capacity, which is not conducive to heat transfer. Thus, the outlet water temperature of DUBHE will decrease with the increase of specific heat capacity and the corresponding soil temperature decay rate will increase. In addition, specific heat capacity has little influence for Q_{total} index, and the increasing rate of the average S/N ratio in level-3 only has a 0.73% difference compared with level-1.

Groundwater seepage strengthens the convection heat transfer outside the borehole and reduces the thermal resistance of soil, which is conducive to heat extraction of DUBHE. The average S/N ratio of T_{out} and Q_{total} under the parallel direction (from the descending well to the ascending well) are 29.85 °C(S/N=29.50) and 180.06 TJ(S/N=45.11), which are lower than the other seepage directions. Moreover, the average S/N ratio of D_{soil} under the parallel direction is 13.6% (S/N= 17.32), which is the worst among all the three seepage directions. It means that the enhancement effect of heat extraction performance with the parallel direction of seepage is the weakest. Owing to the existence of groundwater seepage, the heat stored in the remote soil will be transported to the surrounding area of the horizontal borehole of DUBHE. Therefore, the vertical seepage direction will have a higher heat supply from the remote subsurface and has the best heat extraction enhancement, which is better than the parallel and counter directions. As for the Darcy velocity, the S/N ratios of T_{out}, Q_{total}, and D_{soil} have an increment with the increase of Darcy velocity. When the Darcy velocity is 2×10^{-9} m/s, the average S/N ratios of the three indicators are 29.50, 45.14, and 17.26 respectively. Then the Darcy velocity improves to 2×10^{-7} m/s, the increasing rates of average S/N ratio are just 0.20%, 0.66%, and 0.51% respectively. It is worth noting that Darcy velocity can indeed enhance the heat extraction performance of DUBHE, but the benefit is not obvious within the typical range of groundwater seepage velocity in northern China. The results show that both the groundwater flow direction and Darcy velocity will not bring considerable enhancement to the heat extraction performance of DUBHE, which indicates that the heat convection phenomenon is not the dominant process surrounding the horizontal borehole.

Table 4: Average S/N ratios response of T_{out} under five factors and different levels

Scenarios	Parameters					S/N ratio for T_{out} (dB)				
Levels	A	B	C	D	E	A	B	C	D	E
1	28.81	27.77	**30.20**	**30.03**	29.86	29.19	28.87	**29.60**	**29.55**	29.50
2	29.55	29.94	29.92	29.85	29.89	29.41	29.52	29.52	29.50	29.51
3	**31.45**	**32.11**	29.70	29.94	**30.07**	**29.95**	**30.13**	29.45	29.53	**29.56**
Delta	2.64	4.35	0.51	0.19	0.21	0.76	1.26	0.15	0.05	0.06
Rank	2	1	3	5	4	2	1	3	5	4

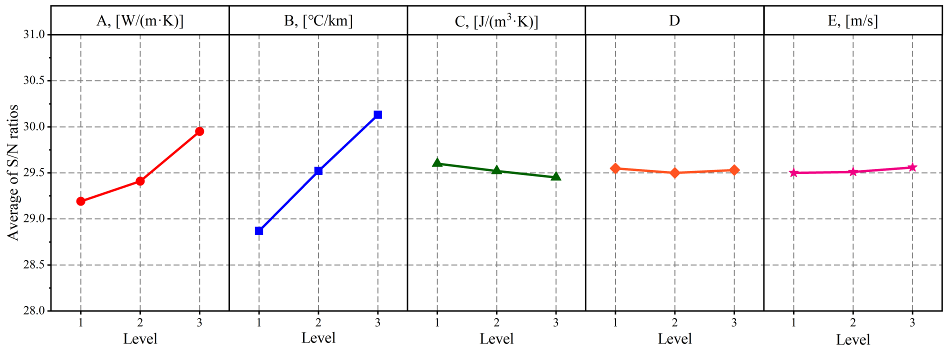

Figure 4: Effect of process parameters on average S/N ratio for T_{out}

Table 5: Average S/N ratios response of Q_{total} under five factors and different levels

Scenarios	Parameters					S/N ratio for Q_{total} (dB)				
Levels	A	B	C	D	E	A	B	C	D	E
1	153.96	137.20	181.61	**184.72**	180.75	43.75	42.75	45.18	**45.33**	45.14
2	173.84	182.82	178.85	180.06	181.09	44.80	45.24	45.05	45.11	45.16
3	**221.18**	**228.96**	**188.52**	184.21	**187.14**	**46.90**	**47.20**	**45.51**	45.31	**45.44**
Delta	67.22	91.76	9.68	4.67	6.39	3.15	4.45	0.46	0.22	0.30
Rank	2	1	3	5	4	2	1	3	5	4

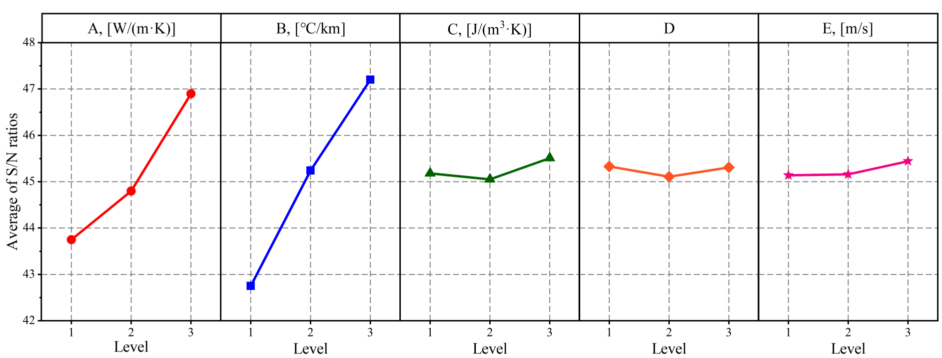

Figure 5: Effect of process parameters on average S/N ratio for Q_{total}

Table 6: Average S/N ratios response of D_{soil} under five factors and different levels

Scenarios	Parameters					S/N ratio for D_{soil} (dB)				
Levels	A	B	C	D	E	A	B	C	D	E
1	**0.132**	**0.136**	0.148	0.137	0.137	**17.57**	**17.32**	16.61	17.29	17.26
2	0.137	0.136	0.142	**0.136**	0.137	17.28	17.30	16.95	**17.32**	17.29
3	0.140	0.137	**0.120**	0.137	**0.136**	17.06	17.28	**18.44**	17.29	**17.35**
Delta	0.008	0.001	0.028	0.001	0.001	0.51	0.04	1.83	0.03	0.09
Rank	2	4	1	5	3	2	4	1	5	3

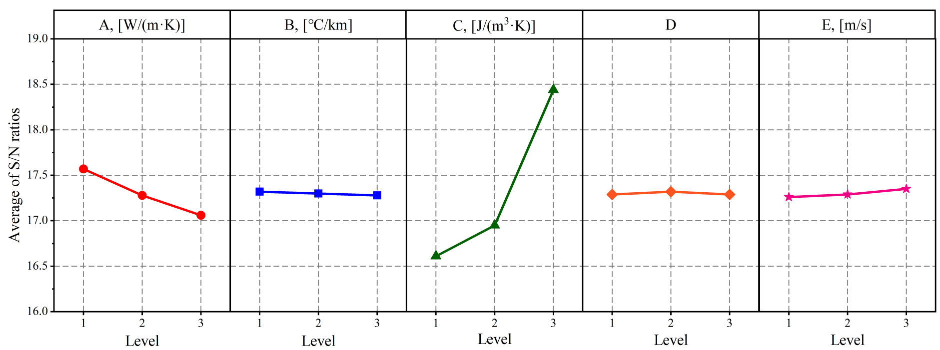

Figure 6: Effect of process parameters on average S/N ratio for D_{soil}

5.2. Analysis of ANOVA method

In the previous section, the S/N ratio is used to evaluate the influence significance of each factor, and the corresponding optimization combinations for three indexes are obtained. ANOVA method will be used to quantify the contribution of each factor on the objective function. If F_{factor} is greater than $F_{0.05}$(95% confidence level), the change of the level of factors has a significant influence on the experimental results, then will be marked as * in our paper.

The contribution degree of five factors and corresponding experimental errors to the three indexes are drawn as a bar chart Fig. 7. It can be clearly seen that B and A (geothermal gradient and thermal conductivity) have significant influence on the objective function of T_{out}, and their contributions are as high as 70.14% and 27.59%. Moreover, it can be shown that C (specific heat capacity) has a certain influence for T_{out} of DUBHE. Compared with the first two parameters, the influence degree of C has little influence, and its contribution degree only accounts for 0.95%. In addition, groundwater flow direction and Darcy velocity have less influence on T_{out} than the first three.

For Q_{total}, the contribution rate of B (geothermal gradient) is the largest, which is 62.10%. Secondly, the influence of A (thermal conductivity) is also obvious for Q_{total}, which has a contribution of 35.18%. This provides a direction for the promotion of deep borehole geothermal heating technology. It is suitable for the promotion of geothermal technology in the abundant geothermal resources, which owns high geothermal gradient and thermal conductivity.

The geological parameters that affect the D_{soil} are C and A (specific heat capacity and thermal conductivity), which contribute 92.41% and 6.74% respectively. It shows that the thermal diffusivity will directly affect the temperature decay rate and temperature recovery of subsurface. The influence of the other three parameters B, D, and E (geothermal gradient, groundwater flow direction, and Darcy velocity) on D_{soil} are less than that of the first two. In scientific research and engineering application, thermal interaction within the borehole array caused by thermal diffusion should be fully considered for system design in order to give reasonable borehole spacing.

Table 7: Results of ANOVA for DUBHE

Variance source	Degree of freedom (DOF)	Sum of squares (SS)	Mean square (MS)	F ratio	$F_{0.05}$	Contribution rate (%)
T_{out}						
A	2	22.29	11.15	97.14	4.74	**27.59***
B	2	56.68	28.34	246.99	4.74	**70.14***
C	2	0.77	0.38	3.35	4.74	0.95
D	2	0.10	0.05	0.45	4.74	0.13
E	2	0.16	0.08	0.69	4.74	0.20
Error	7	0.80	0.11			0.99
Total	17	80.81				100
Q_{total}						
A	2	14310.15	7155.07	87.50	4.74	**35.18***
B	2	25258.20	12629.10	154.44	4.74	**62.10***
C	2	298.12	149.06	1.82	4.74	0.74
D	2	78.47	39.24	0.48	4.74	0.19
E	2	155.15	77.58	0.95	4.74	0.38
Error	7	572.41	81.77			1.41
Total	17	40672.51				100
D_{soil}						
A	2	0.192‰	0.096‰	41.18	4.74	**6.74***
B	2	0.001‰	0.001‰	0.26	4.74	0.04
C	2	2.626‰	1.313‰	564.41	4.74	**92.41***
D	2	0.001‰	0.0003‰	0.14	4.74	0.02
E	2	0.006‰	0.003‰	1.28	4.74	0.21
Error	7	0.016‰	0.002‰			0.58
Total	17	2.842‰				100

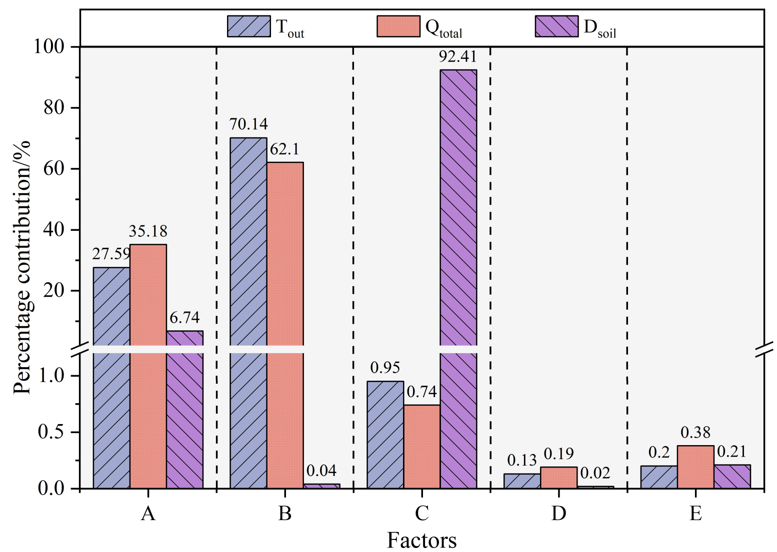

Figure 7: Contribution rates of various factors to evaluation parameters for heat exchange performance

5.3. Analysis of matrix method

Section 5.1 analyzes the proposed three objective function, the optimal combination for T_{out} indicator is $A_3B_3C_1D_1E_3$, and the optimal combination is $A_3B_3C_3D_1E_3$ in view of Q_{total}, the optimal combination for D_{soil} is $A_1B_1C_3D_2E_3$. The previous analysis does not answer the question about what is the comprehensive optimal combination in view of the three indicators. Thus, this section uses the matrix-analytic method [56] to determine the comprehensive optimization combination.

The matrix-analytic method decomposes the weight matrix into three-layer structure models and matrix [57]. The weight matrix of indexes is obtained by multiplying each layer matrix, and the level weight of factors is calculated, so as to determine the optimal combination under comprehensive indexes. The specific expression is as follows:

$$W = MTS \tag{10}$$

Where, W is the weight matrix, M is the tested index layer matrix, T is the factor layer matrix and S is the level matrix.

The calculated result of the weight matrix is presented in this section. Also, the detailed calculation process and results of the weight matrix are shown in section 8 for interested readers.

$$W=\frac{(W_1+W_2+W_3)}{3}=\frac{1}{3}(\begin{bmatrix}0.1062\\0.1089\\0.1159\\0.1683\\0.1815\\0.1946\\0.0213\\0.0211\\0.0209\\0.0076\\0.0076\\0.0076\\0.0089\\0.0089\\0.0089\end{bmatrix}+\begin{bmatrix}0.1036\\0.1170\\0.1489\\0.1262\\0.1682\\0.2106\\0.0177\\0.0174\\0.0183\\0.0086\\0.0084\\0.0086\\0.0117\\0.0117\\0.0121\end{bmatrix}+\begin{bmatrix}0.0704\\0.0681\\0.0664\\0.0053\\0.0053\\0.0053\\0.2218\\0.2306\\0.2735\\0.0040\\0.0040\\0.0040\\0.0118\\0.0119\\0.0119\end{bmatrix})=\begin{bmatrix}0.0934\\0.0980\\\mathbf{0.1104}\\0.0999\\0.1183\\\mathbf{0.1368}\\0.0869\\0.0897\\\mathbf{0.1043}\\0.0067\\0.0066\\\mathbf{0.0067}\\0.0108\\0.0108\\\mathbf{0.0110}\end{bmatrix}=\begin{bmatrix}A_1\\A_2\\A_3\\B_1\\B_2\\B_3\\C_1\\C_2\\C_3\\D_1\\D_2\\D_3\\E_1\\E_2\\E_3\end{bmatrix}$$

Assuming that the weight of T_{out}, Q_{total} and D_{soil} are 1/3 respectively, the final optimized combination is $A_3B_3C_3D_3E_3$ by integrating the three evaluation indexes.

6. Discussion

6.1. Case study of carbon emission reduction

According to the previous results, we can find that thermal conductivity, geothermal gradient, and specific heat capacity are three dominant geological factors that affect the long-term performance of DUBHE. In order to intuitively discuss the potential of carbon emission reduction of DUBHE compared with traditional heating forms, this section sets three scenarios based on the actual geological characteristics. The geothermal gradient of the three scenarios increases gradually, and the detailed features are shown in Table 8.

Table 8: List of three simulated scenarios and features

Scenario	Geological formation	Depth	Thermal conductivity	Geothermal gradient	Specific heat capacity
		m	W m^{-1} K^{-1}	°C km^{-1}	J m^{-3} K^{-1}
A [58]	Formation 1	0-636	1.8	28.5	2.45×10^6
	Formation 2	636-1198	2.6		2.94×10^6
	Formation 3	1198-1910	3.5		1.96×10^6
	Formation 4	1910-2500	5.3		2.28×10^6
B [59]	Formation 1	0-418	1.042	30	3.73×10^6
	Formation 2	418-1030	2.7		2.31×10^6
	Formation 3	1030-1530	2.58		2.35×10^6
	Formation 4	1530-2295	2.53		2.31×10^6
	Formation 5	2295-2500	2.31		2.23×10^6
C [60]	Formation 1	0-420	0.921	33.5	1.29×10^6
	Formation 2	420-1000	1.8		2.45×10^6
	Formation 3	1000-1580	2.6		2.94×10^6
	Formation 4	1580-2000	3.5		1.96×10^6
	Formation 5	2000-2500	5.3		2.28×10^6

According to Fig. 8, the outlet water temperature and heat extraction of DUBHE in the three scenarios gradually decrease when the boundary condition is set as the constant inflow temperature type. They go through a stage of descending, a period of transition, and a stable stage. The outlet water temperature at the end of one heating season is arranged in order of size as 26.51, 24.26, and 19.92°C, corresponding to Scenario_C, Scenario_A, and Scenario_B. It is worth noting that although the geothermal gradient of Scenario_B is slightly larger than that of Scenario_A, the outlet water temperature of Scenario_B is lower than that of Scenario_A. The main reason for this phenomenon is that thermal conductivity occupies an obvious advantage. According to the Q_{total} index mentioned above, the simulation results of three scenarios are 274.34 (Scenario_C), 247.80 (Scenario_A) and 191.39 TJ (Scenario_B) respectively.

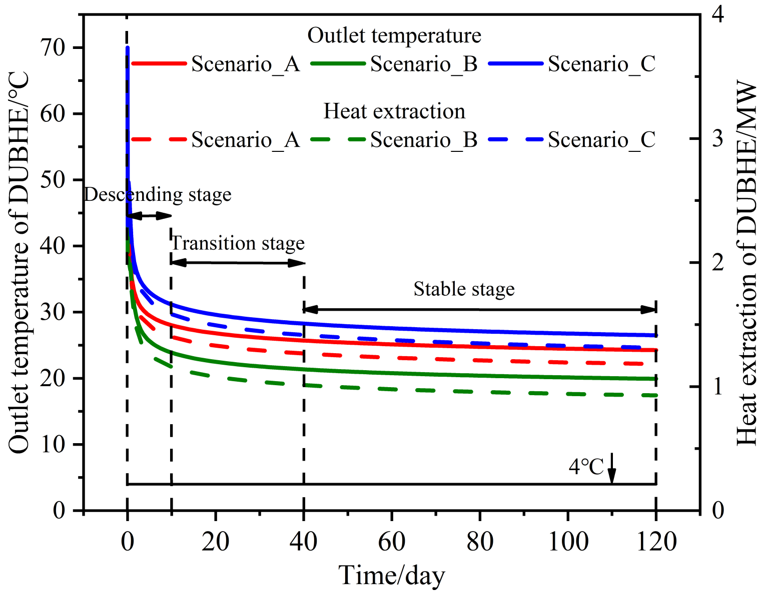

Figure 8: Outlet temperature and heat extraction capacity of DUBHE under three scenarios

To explore the environmental benefits of deep borehole geothermal heating technology, the carbon reduction potential of DUBHE is assessed based on long-term dynamic heat extraction performance. Assuming that the thermal efficiency of the coal-fired boiler is 85%, the carbon emission reduction potential of three scenarios can be calculated. With the highest geothermal gradient and soil thermal conductivity, Scenario_C has the best performance in carbon emission reduction, while Scenario_B with the lowest thermal conductivity has the lowest emission reduction. During the 20 heating seasons, the average value of emission reduction for the three scenarios can be calculated, which are 9559.75 tons of standard coal, 25390.71 tons of carbon dioxide emission, 81.26 tons of sulfur dioxide emission, 149.04 tons of nitrogen oxide emission, and 91.68 tons of dust emission. It can be seen that the carbon emission reduction potential of the DUBHE system is considerable. It is worth vigorously promoting this kind of heating technology in the area with abundant geothermal resources to contribute significantly to a green and sustainable future.

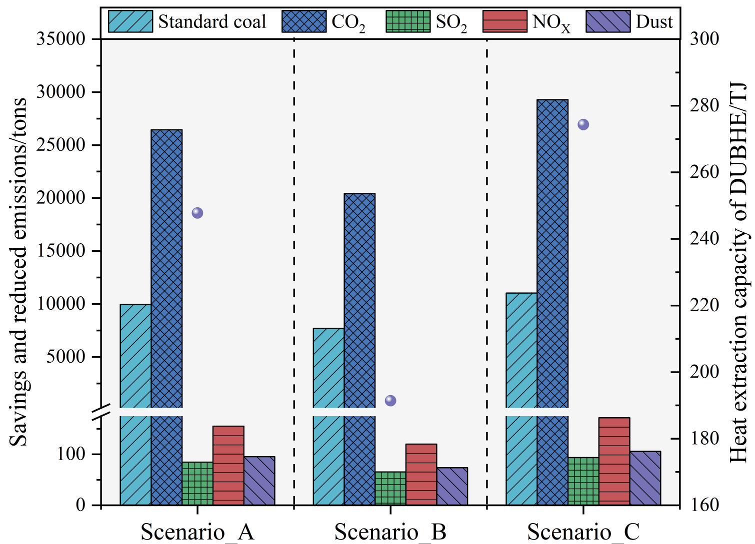

Figure 9: Corresponding carbon reduction amount of DUBHE under the same design parameters

6.2. Future work

Geothermal energy, as renewable energy with great development potential in the 21st century [61], has been widely used in the world. Right now, geothermal energy is basically used for power generation, building heating, and agriculture. In 2019, the global wind power with a total installed capacity of 6.5 million kilowatts [62], given that clean energy power has become the future trend. Combining the energy storage concept and the deep borehole geothermal heating technology organically can be an important goal of the development of renewable energy. In the future research, we will focus on the combination of DUBHE and energy storage technology, and investigate the feasibility of coupled energy storage and the DUBHE system, so as to provide new ideas for the development of energy storage technology in the future.

7. Conclusions

The main purpose of this study is to evaluate the heat extraction performance of DUBHE with different geological parameters during long-term operation. 3D numerical heat transfer models of DUBHE are built using OpenGeoSys software and the Taguchi method is introduced for this purpose. Thermal conductivity, geothermal gradient, specific heat capacity, groundwater flow direction, and Darcy velocity five geological parameters and corresponding three levels are considered and 18 sets of orthogonal simulation conditions $L_{18}(3^5)$ is made. Using the S/N ratio and ANOVA method, the optimal combination and contribution rate of each influencing factor have been identified and analyzed in detail. To be more specific:

(i) Determined by the Taguchi method, the influence for T_{out} indexes follows the sequence of geothermal gradient (70.14%), thermal conductivity (27.59%), specific heat capacity (0.95%), Darcy velocity (0.20%), and groundwater flow direction (0.13%). The calculation of ANOVA method indicates that geothermal gradient and thermal conductivity play a vital role in assessing the value of Q_{total} with 62.10% and 35.18% of the contribution rate respectively. The impact of specific heat capacity (0.74%), groundwater flow direction (0.38%), and Darcy velocity (0.19%) can be nearly neglected for Q_{total} of DUBHE. And for the D_{soil} index, the influence degree is in the order of specific heat capacity, thermal conductivity, Darcy velocity, geothermal gradient, and groundwater flow direction, along with contribution rates of 92.41%, 6.74%, 0.21%, 0.04%, and 0.02% respectively.

(ii) By integrating T_{out}, Q_{total}, and D_{soil} indexes with the assumption of average weight proportion, the final optimized combination is $A_3B_3C_3D_3E_3$. The optimized values of thermal conductivity, geothermal gradient, specific heat capacity, groundwater flow direction, and Darcy velocity are level-3 (detailed parameters are shown in Table 2). According to the optimized combination of three indexes, the T_{out} reaches 33.92 °C and the Q_{total} is 284.08 TJ under long-term operation conditions, while the D_{soil} is 12.66% by using the optimal parameters set.

(iii) The popularization of DUBHE has certain environmental friendliness and benefits to the environment considering decarbonization. In the case study, the quantification of the reduction potential of carbon emission shows that 1 TJ of heat provided by DUBHE is equivalent to a reduction of 40.19 tons of standard coal. Moreover, 106.75 tons of CO_2 emission, 341.65 kg of SO_2 emission, 626.62 kg of NO_x emission, and 385.46 kg of dust emission can be reduced for 1 TJ of heat provided by DUBHE.

Our work shows that the three geological parameters of geothermal gradient, thermal conductivity, and specific heat capacity of soil have significant influences on the long-term performance of DUBHE. Moreover, the groundwater seepage also has certain effects on the long-term performance of the DUBHE system so it should be carefully considered and evaluated in the system design. Therefore, sufficient geological investigation should be adopted in the early stage of the geothermal projects to ensure the long-term sustainability of DUBHE. Comprehensive simulation tools such as OpenGeoSys can be introduced to conduct the optimization in the application of deep geothermal energy.

8. Appendix

$$M_1 = \begin{bmatrix} 28.81 & 0 & 0 & 0 & 0 \\ 29.55 & 0 & 0 & 0 & 0 \\ 31.45 & 0 & 0 & 0 & 0 \\ 0 & 27.77 & 0 & 0 & 0 \\ 0 & 29.94 & 0 & 0 & 0 \\ 0 & 32.11 & 0 & 0 & 0 \\ 0 & 0 & 30.20 & 0 & 0 \\ 0 & 0 & 29.92 & 0 & 0 \\ 0 & 0 & 29.70 & 0 & 0 \\ 0 & 0 & 0 & 30.03 & 0 \\ 0 & 0 & 0 & 29.85 & 0 \\ 0 & 0 & 0 & 29.94 & 0 \\ 0 & 0 & 0 & 0 & 29.86 \\ 0 & 0 & 0 & 0 & 29.89 \\ 0 & 0 & 0 & 0 & 30.07 \end{bmatrix}$$

$$T_1 = \begin{bmatrix} 0.011 & 0 & 0 & 0 & 0 \\ 0 & 0.011 & 0 & 0 & 0 \\ 0 & 0 & 0.011 & 0 & 0 \\ 0 & 0 & 0 & 0.011 & 0 \\ 0 & 0 & 0 & 0 & 0.011 \end{bmatrix}$$

$$S_1^T = \begin{bmatrix} 0.335 & 0.551 & 0.064 & 0.023 & 0.027 \end{bmatrix}$$

$$M_2 = \begin{bmatrix} 153.96 & 0 & 0 & 0 & 0 \\ 173.84 & 0 & 0 & 0 & 0 \\ 221.18 & 0 & 0 & 0 & 0 \\ 0 & 137.20 & 0 & 0 & 0 \\ 0 & 182.82 & 0 & 0 & 0 \\ 0 & 228.96 & 0 & 0 & 0 \\ 0 & 0 & 181.61 & 0 & 0 \\ 0 & 0 & 178.85 & 0 & 0 \\ 0 & 0 & 188.52 & 0 & 0 \\ 0 & 0 & 0 & 184.72 & 0 \\ 0 & 0 & 0 & 180.06 & 0 \\ 0 & 0 & 0 & 184.21 & 0 \\ 0 & 0 & 0 & 0 & 180.75 \\ 0 & 0 & 0 & 0 & 181.09 \\ 0 & 0 & 0 & 0 & 187.14 \end{bmatrix}$$

$$T_2 = \begin{bmatrix} 0.0018 & 0 & 0 & 0 & 0 \\ 0 & 0.0018 & 0 & 0 & 0 \\ 0 & 0 & 0.0018 & 0 & 0 \\ 0 & 0 & 0 & 0.0018 & 0 \\ 0 & 0 & 0 & 0 & 0.0018 \end{bmatrix}$$

$$S_2^T = \begin{bmatrix} 0.374 & 0.511 & 0.054 & 0.026 & 0.036 \end{bmatrix}$$

$$M_3 = \begin{bmatrix} 7.56 & 0 & 0 & 0 & 0 \\ 7.31 & 0 & 0 & 0 & 0 \\ 7.13 & 0 & 0 & 0 & 0 \\ 0 & 7.34 & 0 & 0 & 0 \\ 0 & 7.33 & 0 & 0 & 0 \\ 0 & 7.31 & 0 & 0 & 0 \\ 0 & 0 & 6.77 & 0 & 0 \\ 0 & 0 & 7.04 & 0 & 0 \\ 0 & 0 & 8.35 & 0 & 0 \\ 0 & 0 & 0 & 7.32 & 0 \\ 0 & 0 & 0 & 7.34 & 0 \\ 0 & 0 & 0 & 7.32 & 0 \\ 0 & 0 & 0 & 0 & 7.29 \\ 0 & 0 & 0 & 0 & 7.32 \\ 0 & 0 & 0 & 0 & 7.37 \end{bmatrix}$$

$$T_3 = \begin{bmatrix} 0.045 & 0 & 0 & 0 & 0 \\ 0 & 0.045 & 0 & 0 & 0 \\ 0 & 0 & 0.045 & 0 & 0 \\ 0 & 0 & 0 & 0.045 & 0 \\ 0 & 0 & 0 & 0 & 0.045 \end{bmatrix}$$

$$S_3^T = \begin{bmatrix} 0.207 & 0.016 & 0.728 & 0.012 & 0.036 \end{bmatrix}$$

$$W = \frac{(W_1 + W_2 + W_3)}{3} = \frac{1}{3}\left(\begin{bmatrix} 0.1062 \\ 0.1089 \\ 0.1159 \\ 0.1683 \\ 0.1815 \\ 0.1946 \\ 0.0213 \\ 0.0211 \\ 0.0209 \\ 0.0076 \\ 0.0076 \\ 0.0076 \\ 0.0089 \\ 0.0089 \\ 0.0089 \end{bmatrix} + \begin{bmatrix} 0.1036 \\ 0.1170 \\ 0.1489 \\ 0.1262 \\ 0.1682 \\ 0.2106 \\ 0.0177 \\ 0.0174 \\ 0.0183 \\ 0.0086 \\ 0.0084 \\ 0.0086 \\ 0.0117 \\ 0.0117 \\ 0.0121 \end{bmatrix} + \begin{bmatrix} 0.0704 \\ 0.0681 \\ 0.0664 \\ 0.0053 \\ 0.0053 \\ 0.0053 \\ 0.2218 \\ 0.2306 \\ 0.2735 \\ 0.0040 \\ 0.0040 \\ 0.0040 \\ 0.0118 \\ 0.0119 \\ 0.0119 \end{bmatrix} \right) = \begin{bmatrix} 0.0934 \\ 0.0980 \\ \mathbf{0.1104} \\ 0.0999 \\ 0.1183 \\ \mathbf{0.1368} \\ 0.0869 \\ 0.0897 \\ \mathbf{0.1043} \\ 0.0067 \\ 0.0066 \\ \mathbf{0.0067} \\ 0.0108 \\ 0.0108 \\ \mathbf{0.0110} \end{bmatrix} = \begin{bmatrix} A_1 \\ A_2 \\ A_3 \\ B_1 \\ B_2 \\ B_3 \\ C_1 \\ C_2 \\ C_3 \\ D_1 \\ D_2 \\ D_3 \\ E_1 \\ E_2 \\ E_3 \end{bmatrix}$$

CRediT authorship contribution statement

Jinghua Jiang: Conceptualization, Methodology, Software, Validation, Writing - Original Draft, Visualization. **Fenghao Wang:** Conceptualization, Formal analysis, Project administration, Funding acquisition, Supervision. **Xiong Yang:** Methodology, Software, Visualization. **Yuping Zhang:** Investigation, Data curation. **Jiewen Deng:** Methodology, Investigation. **Qingpeng Wei:** Methodology, Formal analysis. **Wanlong Cai:** Conceptualization, Software, Validation, Investigation, Writing - Review & Editing. **Chaofan Chen:** Methodology, Software, Writing - Review & Editing, Resources.

Declaration of competing interest

The authors declare that they have no known competing financial interests or personal relationships that could have appeared to influence the work reported in this paper.

Acknowledgements

This research is financially supported by the Key Research and Development Project of Shaanxi Province (2020ZDLSF06-08), as well as the Open Project of Key Laboratory of Coal Resources Exploration and Comprehensive Utilization (KF2021-1), which is funded by the Chinese Ministry of Natural Resources.

References

[1] C.-W. Su, K. Khan, M. Umar, W. Zhang, Does renewable energy redefine geopolitical risks?, Energy Policy 158 (2021) 112566.

[2] Z. Caineng, B. XIONG, X. Huaqing, D. ZHENG, G. Zhixin, W. Ying, L. JIANG, P. Songqi, W. Songtao, The role of new energy in carbon neutral, Petroleum exploration and development 48 (2021) 480–491.

[3] B. Wang, Q. Wang, Y.-M. Wei, Z.-P. Li, Role of renewable energy in china's energy security and climate change mitigation: An index decomposition analysis, Renewable and sustainable energy reviews 90 (2018) 187–194.

[4] Q. Fu, Z. Han, J. Chen, Y. Lu, H. Wu, Y. Wang, Applications of reinforcement learning for building energy efficiency control: A review, Journal of Building Engineering (2022) 104165.

[5] D. D'Agostino, L. Mazzarella, What is a nearly zero energy building? overview, implementation and comparison of definitions, Journal of Building Engineering 21 (2019) 200–212.

[6] D. Mariano-Hernández, L. Hernández-Callejo, A. Zorita-Lamadrid, O. Duque-Pérez, F. S. García, A review of strategies for building energy management system: Model predictive control, demand side management, optimization, and fault detect & diagnosis, Journal of Building Engineering 33 (2021) 101692.

[7] T. Harputlugil, P. de Wilde, The interaction between humans and buildings for energy efficiency: A critical review, Energy Research & Social Science 71 (2021) 101828.

[8] J. Lin, B. Lin, The actual heating energy conservation in china: evidence and policy implications, Energy and Buildings 190 (2019) 195–201.

[9] D. Balsalobre-Lorente, O. M. Driha, N. C. Leitão, M. Murshed, The carbon dioxide neutralizing effect of energy innovation on international tourism in eu-5 countries under the prism of the ekc hypothesis, Journal of Environmental Management 298 (2021) 113513.

[10] L. Zhang, S. Chen, C. Zhang, Geothermal power generation in china: Status and prospects, Energy Science & Engineering 7 (2019) 1428–1450.

[11] L. Rybach, R. Hopkirk, Shallow and deep borehole heat exchangers—achievements and prospects, in: Pro. World Geothermal Congress, volume 1995, 1995, pp. 2133–2139.

[12] K. Morita, W. S. Bollmeier, H. Mizogami, An experiment to prove the concept of the downhole coaxial heat exchanger (dche) in hawaii, Geothermal Resources Council Transactions 16 (1992).

[13] L. Dijkshoorn, S. Speer, R. Pechnig, Measurements and design calculations for a deep coaxial borehole heat exchanger in aachen, germany, International Journal of Geophysics 2013 (2013).

[14] Z. Wang, F. Wang, J. Liu, Z. Ma, E. Han, M. Song, Field test and numerical investigation on the heat transfer characteristics and optimal design of the heat exchangers of a deep borehole ground source heat pump system, Energy conversion and management 153 (2017) 603–615.

[15] J. Deng, Q. Wei, M. Liang, S. He, H. Zhang, Field test on energy performance of medium-depth geothermal heat pump systems (md-ghps), Energy and Buildings 184 (2019) 289–299.

[16] X. Song, G. Wang, Y. Shi, R. Li, Z. Xu, R. Zheng, Y. Wang, J. Li, Numerical analysis of heat extraction performance of a deep coaxial borehole heat exchanger geothermal system, Energy 164 (2018) 1298–1310.

[17] W. Cai, F. Wang, J. Liu, Z. Wang, Z. Ma, Experimental and numerical investigation of heat transfer performance and sustainability of deep borehole heat exchangers coupled with ground source heat pump systems, Applied Thermal Engineering 149 (2019) 975–986.

[18] C. Chen, H. Shao, D. Naumov, Y. Kong, K. Tu, O. Kolditz, Numerical investigation on the performance, sustainability, and efficiency of the deep borehole heat exchanger system for building heating, Geothermal Energy 7 (2019) 1–26.

[19] C. Li, Y. Guan, X. Wang, C. Zhou, Y. Xun, L. Gui, Experimental and numerical studies on heat transfer characteristics of vertical deep-buried u-bend pipe in intermittent heating mode, Geothermics 79 (2019) 14–25.

[20] X. Z. Y. Han, C. Sun, Principle and utilization of medium-deep u-shaped geothermal heating technology, Energy Conservation Technology 5 (2020) 93–94 (in chinese).

[21] Y. Mingzhi, L. Wei, Z. Fangfang, Z. Wenke, C. Ping, F. Zhaohong, A novel model and heat extraction capacity of mid-deep buried u-bend pipe ground heat exchangers, Energy and Buildings 235 (2021) 110723.

[22] C. Chen, W. Cai, D. Naumov, K. Tu, H. Zhou, Y. Zhang, O. Kolditz, H. Shao, Numerical investigation on the capacity and efficiency of a deep enhanced u-tube borehole heat exchanger system for building heating, Renewable Energy 169 (2021) 557–572.

[23] C. Guan, Z. Fang, W. Zhang, H. Yao, Y. Man, M. Yu, Dynamic heat transfer analysis on the new u-type medium-deep borehole ground heat exchanger, Frontiers in Energy Research (2022) 271.

[24] Y. Noorollahi, M. Pourarshad, S. Jalilinasrabady, H. Yousefi, Numerical simulation of power production from abandoned oil wells in ahwaz oil field in southern iran, Geothermics 55 (2015) 16–23.

[25] R. A. Caulk, I. Tomac, Reuse of abandoned oil and gas wells for geothermal energy production, Renewable energy 112 (2017) 388–397.

[26] X. Hu, J. Banks, Y. Guo, W. V. Liu, Retrofitting abandoned petroleum wells as doublet deep borehole heat exchangers for geothermal energy production—a numerical investigation, Renewable Energy 176 (2021) 115–134.

[27] S. Gharibi, E. Mortezazadeh, S. J. H. A. Bodi, A. Vatani, Feasibility study of geothermal heat extraction from abandoned oil wells using a u-tube heat exchanger, Energy 153 (2018) 554–567.

[28] P. J. S. Tang, P. Li, Numerical simulation of high efficiency heat transfer rule in horizontal section of u-shaped geothermal well in guanzhong area, Journal of Xi'an University of Science and Technology (2019) 8 (in chinese).

[29] X. Wang, Study on heat transfer performance of middle deep u-tube borehole heat exchanger, District Heating 5 (2021) 20–24+43 (in chinese).

[30] C. Li, Y. Guan, Y. Feng, C. Jiang, S. Zhen, X. Su, Comparison of influencing factors and level optimization for heating through deep-buried pipe based on taguchi method, Geothermics 91 (2021) 102045.

[31] G. Jia, Z. Ma, Z. Xia, J. Wang, Y. Zhang, L. Jin, Investigation of the horizontally-butted borehole heat exchanger based on a semi-analytical method considering groundwater seepage and geothermal gradient, Renewable Energy 171 (2021) 447–461.

[32] T. Sivasakthivel, K. Murugesan, P. Sahoo, Optimization of ground heat exchanger parameters of ground source heat pump system for space heating applications, Energy 78 (2014) 573–586.

[33] G. Murali, R. Fediuk, A taguchi approach for study on impact response of ultra-high-performance polypropylene fibrous cementitious composite, Journal of Building Engineering 30 (2020) 101301.

[34] K. Zhou, J. Mao, Y. Li, J. Xiang, Parameters optimization of borehole and internal thermal resistance for single u-tube ground heat exchangers using taguchi method, Energy Conversion and Management 201 (2019) 112177.

[35] S. Kumar, K. Murugesan, Optimization of geothermal interaction of a double u-tube borehole heat exchanger for space heating and cooling applications using taguchi method and utility concept, Geothermics 83 (2020) 101723.

[36] N. Jamshidi, A. Mosaffa, Investigating the effects of geometric parameters on finned conical helical geothermal heat exchanger and its energy extraction capability, Geothermics 76 (2018) 177–189.

[37] H.-J. Diersch, D. Bauer, W. Heidemann, W. Rühaak, P. Schätzl, Finite element modeling of borehole heat exchanger systems: Part 1. fundamentals, Computers & Geosciences 37 (2011) 1122–1135.

[38] H.-J. Diersch, D. Bauer, W. Heidemann, W. Rühaak, P. Schätzl, Finite element modeling of borehole heat exchanger systems: Part 2. numerical simulation, Computers & Geosciences 37 (2011) 1136–1147.

[39] S. Chen, F. Witte, O. Kolditz, H. Shao, Shifted thermal extraction rates in large borehole heat exchanger array–a numerical experiment, Applied Thermal Engineering 167 (2020) 114750.

[40] R. Wang, F. Wang, Y. Xue, J. Jiang, Y. Zhang, W. Cai, C. Chen, Numerical study on the long-term performance and load imbalance ratio for medium-shallow borehole heat exchanger system, Energies 15 (2022) 3444.

[41] S. Chen, W. Cai, F. Witte, X. Wang, F. Wang, O. Kolditz, H. Shao, Long-term thermal imbalance in large borehole heat exchangers array–a numerical study based on the leicester project, Energy and Buildings 231 (2021) 110518.

[42] W. Cai, F. Wang, J. Jiang, Z. Wang, J. Liu, C. Chen, Long-term performance evaluation and economic analysis for deep borehole heat exchanger heating system in weihe basin, Frontiers in Earth Science 10 (2022) 806416.

[43] W. Cai, F. Wang, S. Chen, C. Chen, J. Liu, J. Deng, O. Kolditz, H. Shao, Analysis of heat extraction performance and long-term sustainability for multiple deep borehole heat exchanger array: A project-based study, Applied Energy 289 (2021) 116590.

[44] Y. Guan, X. Zhang, C. Liang, W. Wang, Y. Zhang, Regional distribution of rock-soil influences for ground heat exchange of ground-source heat pump in xi'an area, Journal of Northwest University (Natural Science Edition) 46 (2016) 565–572 (in chinese).

[45] T. Kıvak, Optimization of surface roughness and flank wear using the taguchi method in milling of hadfield steel with pvd and cvd coated inserts, Measurement 50 (2014) 19–28.

[46] J. Liu, F. Wang, W. Cai, Z. Wang, C. Li, Numerical investigation on the effects of geological parameters and layered subsurface on the thermal performance of medium-deep borehole heat exchanger, Renewable Energy 149 (2020) 384–399.

[47] S. Rao, G.-Z. Jiang, Y.-J. Gao, S.-B. Hu, J.-Y. Wang, The thermal structure of the lithosphere and heat source mechanism of geothermal field in weihe basin, chinese Journal of Geophysics 59 (2016) 2176–2190.

[48] A. D. Chiasson, S. J. Rees, J. D. Spitler, A preliminary assessment of the effects of groundwater flow on closed-loop ground source heat pump systems, Technical Report, Oklahoma State Univ., Stillwater, OK (US), 2000.

[49] N. Molina-Giraldo, P. Blum, K. Zhu, P. Bayer, Z. Fang, A moving finite line source model to simulate borehole heat exchangers with groundwater advection, International Journal of Thermal Sciences 50 (2011) 2506–2513.

[50] A. Rodhe, J. Seibert, Groundwater dynamics in a till hillslope: flow directions, gradients and delay, Hydrological Processes 25 (2011) 1899–1909.

[51] W. Cai, F. Wang, C. Chen, S. Chen, J. Liu, Z. Ren, H. Shao, Long-term performance evaluation for deep borehole heat exchanger array under different soil thermal properties and system layouts, Energy 241 (2022) 122937.

[52] I. Asiltürk, H. Akkuş, Determining the effect of cutting parameters on surface roughness in hard turning using the taguchi method, Measurement 44 (2011) 1697–1704.

[53] M. Mamourian, K. M. Shirvan, R. Ellahi, A. Rahimi, Optimization of mixed convection heat transfer with entropy generation in a wavy surface square lid-driven cavity by means of taguchi approach, International Journal of Heat and Mass Transfer 102 (2016) 544–554.

[54] M. Sarıkaya, A. Güllü, Multi-response optimization of minimum quantity lubrication parameters using taguchi-based grey relational analysis in turning of difficult-to-cut alloy haynes 25, Journal of Cleaner Production 91 (2015) 347–357.

[55] N. Celik, G. Pusat, E. Turgut, Application of taguchi method and grey relational analysis on a turbulated heat exchanger, International Journal of Thermal Sciences 124 (2018) 85–97.

[56] J. L. Liu, A. G. Wu, Analysis of manufacturing systems with parallel unreliable machines and finite buffer based on matrix-analytic method, in: Applied Mechanics and Materials, volume 130, Trans Tech Publ, 2012, pp. 479–482.

[57] X. Wei, B. Xue, Q. Zhao, Optimization design of the stability for the plunger assembly of oil pumps based on multi-target orthogonal test design, Journal of Hebei University of Engineering (Natural Science Edition) 27 (2010) 95–99.

[58] J. Deng, Q. Wei, S. He, M. Liang, H. Zhang, Simulation analysis on the heat performance of deep borehole heat exchangers in medium-depth geothermal heat pump systems, Energies 13 (2020) 754.

[59] W. Zhang, J. Wang, F. Zhang, W. Lu, P. Cui, C. Guan, M. Yu, Z. Fang, Heat transfer analysis of u-type deep borehole heat exchangers of geothermal energy, Energy and Buildings 237 (2021) 110794.

[60] P. Zhonghe, L. Ji, C. Yuanzhi, D. Zhongfeng, T. Jiao, K. Yanlong, L. Yiman, H. Shengbiao, W. Jiyang, Evaluation of geological conditions for the development of deep geothermal energy in china, Earth Science Frontiers 27 (2020) 134.

[61] J. Hou, M. Cao, P. Liu, Development and utilization of geothermal energy in china: Current practices and future strategies, Renewable energy 125 (2018) 401–412.

[62] X. Peng, Z. Liu, D. Jiang, A review of multiphase energy conversion in wind power generation, Renewable and Sustainable Energy Reviews 147 (2021) 111172.